Title	Polarity assessment of thermoresponsive poly(NIPAM-co-NtBA) copolymer films using fluorescence methods.
Author(s)	Szczupak, Boguslaw; Ryder, Alan G.; Togashi, Denisio M.; Rochev, Yuri A.; Gorelov, Alexander; Glynn, Thomas J.
Publication Date	2010
Publication Information	B. Szczupak, A.G. Ryder, D.M. Togashi, Y.A. Rotchev, A.S. Klymchenko, A. Gorelov, and T.J. Glynn (2010). Polarity assessment of thermoresponsive poly(NIPAM-co-NtBA) copolymer films using fluorescence methods. Journal of Fluorescence, 20(3), 719-731, (2010).
Publisher	Springer
Link to publisher's version	http://dx.doi.org/10.1007/s10895-010-0613-5
Item record	http://hdl.handle.net/10379/1201

Polarity assessment of thermoresponsive poly(NIPAM-co-NtBA) copolymer films using fluorescence methods.

Boguslaw Szczupak,[a,e] Alan G. Ryder,[a,*] Denisio M. Togashi,[a]

Andrey S. Klymchenko,[c] Yuri A. Rochev,[b] Alexander Gorelov,[d] and Thomas J. Glynn.[e]

[a] Nanoscale Biophotonics Laboratory, School of Chemistry, National University of Ireland, Galway, Galway, Ireland.

[b] National Centre for Biomedical Engineering Sciences, National University of Ireland, Galway, Galway, Ireland.

[c] Laboratoire de Biophotonique et Pharmacologie, UMR 7213 CNRS, Faculté de Pharmacie, Université de Strasbourg, Illkirch, France..

[d] Department of Chemistry, University College Dublin, Ireland.

[e] School of Physics, National University of Ireland, Galway, Galway, Ireland

Abstract

The *in-situ*, non-contact, and non-destructive measurement of the physicochemical properties such as the polarity of thin (nm to μm), hydrophilic polymer films is desirable in many areas of polymer science. Polarity is a complex factor and encompasses a range of non-covalent interactions including dipolarity/polarizability and hydrogen bonding. A polarity measurement method based on fluorescence would be ideal, but the key challenge is to identify suitable probes which can accurately measure specific polarity related parameters. In this manuscript we assess a variety of fluorophores for measuring the polarity of a series of relatively hydrophilic, thermoresponsive N-isopropylacrylamide/N-tert-butylacrylamide (NIPAM/NtBA) copolymers. The emission properties of both pyrene and 3-Hydroxyflavone (3-HF) based fluorophores were measured in dry polymer films. In the case of pyrene, a relatively weak, linear relationship between polymer composition and the ratio of the first to the third vibronic band of the emission spectrum (I_1/I_3) is observed, but pyrene emission is very sensitive to temperature and thus not suitable for robust polarity measurements. The 3-HF fluorophores which can undergo an excited-state intramolecular proton transfer (ESIPT)

reaction have a dual band fluorescence emission that exhibits strong solvatochromism. Here we used 4'-diethylamino-3-hydroxyflavone (FE), 5,6-benzo-4'-diethylamino-3-hydroxyflavone (BFE), and 4´-diethylamino-3-hydroxy-7-methoxyflavone (MFE)). The log ratio of the dual band fluorescence emission (log (I_N^*/I_T^*)) of 3-HF doped, dry, NIPAM-NtBA copolymer films were found to depend linearly on copolymer composition, with increasing hydrophobicity (greater NtBA fraction) leading to a decrease in the value of log (I_N^*/I_T^*). However, the ESIPT process in the polymer matrix was found to be irreversible, non-equilibrated and occurs over a much longer timescale in comparison to the results previously reported for liquid solvents.

Introduction

The use of functional coatings based on nanometre to micrometre thick hydrophilic polymer films is becoming more widespread in medical devices and pharmaceutical formulations. These functional, supported polymer coatings can serve as aids to improve implanted device compatibility and/or as reservoirs for local drug delivery [1, 2]. In one such example, manufacturers of coronary stents are developing stents coated with drug-eluting polymers, with a view to achieve local delivery of potential anti-restenosis therapies [1]. These polymer coatings are relatively thin (~20 to ~100 µm) and formed on small and complex geometries (the typical size of a coronary stent is 15 x 3 mm) and this combination generates significant problems for *in-situ* polymer film analysis. The drug elution rate, long-term storage, device efficacy, and hence regulatory issues are all dependent on the physicochemical properties of the polymer film coating. Understanding these properties in detail is important from the standpoint of predicting how thin polymer films will behave for different biomedical applications under physiological conditions. For example, changes in polymer polarity will have significant impact on the water uptake and retention rates, which in turn, can affect the mechanical and chemical properties of the polymers and impact the manufacturing processes.

---

*Corresponding author: alan.ryder@nuigalway.ie; phone 353-91-492943; fax 353-91-494596; web: http://www.nuigalway.ie/nanoscale/

The analysis of thin polymer films for biomedical applications typically involves the analysis of two separate domains - the polymer surface, and the bulk film. For *in-situ* analysis of the bulk properties of polymer films, various optical techniques can be employed including vibrational, fluorescence, and UV-Visible absorption spectroscopy [3, 4]. In particular, fluorescence spectroscopy has received considerable interest due to its high sensitivity, selectivity, and non-destructive characteristics. However, for fluorescence methods to be useful for characterising polymer films one must overcome problems such as photobleaching, excitation source instabilities, and local variations in probe concentration. One way in which this can be achieved is by using ratiometric fluorophores, which are, in essence, self-calibrating, and immune to the difficulties associated with the use of single emission band probes. One such class of ratiometric fluorophores that have recently been developed are based on 3-hydroxyflavone (3-HF) [5, 6]. These 3-HF probes operate on the principle of an excited-state intramolecular proton transfer (ESIPT) process and exhibit very strong solvatochromism and electrochromism [7-9]. The dual band emission, in terms of wavelength and relative intensities of the two well-separated emission bands, is sensitive to various aspects of their microenvironment [7]. One of these bands originates from the normal excited state (N*), and the other is due to the ESIPT reaction product tautomer (T*). A number of spectroscopic variables can thus be recorded, each of which is sensitive to different kinds of perturbation of the local environment [7-12]. The most important parameter is the ratio of the emission intensities from the N* and T* excited states, I_{N*}/I_{T*}, which is associated with the relative energies of the N* and T* states [7, 10] and is a very sensitive indicator of solvent polarity [11]. The behaviour of these emission bands as well as the relationship of their intensities depends strongly on probe structure. Changing the chemical structure at the fluorophore core can be used to: adjust the dye to a specific range of solvent polarity, to modulate sensitivity to hydrogen bonding, or to electric fields [6, 12-14]. 4'-Diethylamino-3-hydroxyflavone (FE), 5, 6-benzo-4'-diethylamino-3-hydroxyflavone (BFE), and 4´-diethylamino-3-hydroxy-7-methoxyflavone (MFE) are examples of 3-HF fluorophores. The fluorescence emission of the FE, MFE, and BFE probes are extremely sensitive to the properties of solvent environment [6, 7, 13]. An increase in solvent polarity and hydrogen bonding ability of the solvent environment leads to an increase in the population of the N* form relative to T* form, which is due to a greater dielectric stabilization of N* form [7]. Using the ratio of the intensities of these two forms, it has been possible to correlate changes in polarity and hydrogen bonding in various classes of solvents [7, 13]. However, the

sensitivity profiles of these three dyes are different. BFE, unlike the other two dyes, is nearly insensitive to the H-bond donor ability of protic solvents because of the additional benzene ring [13]. MFE shows more solvent-dependent dual emission in more polar solvents when compared to FE [6]. The use of all these three dyes in the present study should provide a more complete characterization of polymer films in terms of both polarity and specific H-bonding interactions.

In our laboratory we are interested in developing a non-contact, non-destructive and sensitive fluorescence-based methodology for the quantitative analysis of polymer coatings (in particular drug-eluting types). In particular, we are focussing on developing a robust method for gross polymer polarity, i.e. a method that quantifies not only the dipolarity/polarizability aspect but also hydrogen-bonding effects. The polymer system that we are studying is a novel thermoresponsive copolymer system that exhibits Lower Critical Solution Temperatures (LCST) below 32 ºC. The LCST of these poly-N-isopropylacrylamide -N-tert-butylacrylamide (pNIPAM-co-NtBA) thermoresponsive copolymers can be decreased by increasing the NtBA fraction. The importance of this study lies in the fact that these pNIPAM-co-NtBA copolymers are currently being investigated as potential drug elution matrices and for cell culture applications [16-20]. Because these copolymers are relatively hydrophilic and will uptake water, it can be difficult to characterise the materials using conventional techniques like Contact Angle Measurements. There is a need therefore to develop non-contact methods of characterising physiochemical properties so as to inform thin film manufacturing methods.

Here we have incorporated pyrene, FE, MFE, and BFE into a range of different pNIPAM-co-NtBA copolymers in order to evaluate the suitability of these probes to measure gross polymer polarity. A previous, preliminary study showed that the emission properties can be correlated with changes in polymer composition [15]. In this work we elaborate on these findings, study the pyrene scale, and show that the ESIPT process is not reversible and that the emission behaviour in polymers is very different to that observed in solvents.

Experimental

Materials: N-isopropylacrylamide (NIPAM) (97%, Aldrich) and N-tert-butylacrylamide (NtBA) (purum, Fluka Chemie, Switzerland) were recrystallized from n-hexane and acetone, respectively. 2,2'-Azobis(2-methylpropionitrile) (Phase Separation Ltd., U.K.) was

recrystallized from methanol. All solvents were reagent grade and were purified before use [20]. A series of copolymers of N-isopropylacrylamide (NIPAM) and N-tert-butylacrylamide (NtBA) with ratios (*w/w*) of 100:0, 85:15 (*P85*), 65:35 (*P65*), 50:50 (*P50*), and 0:100 were synthesized as described previously [20].   The pNIPAM polymer had an approximate molecular weight of ~100,000. The fluorescence probes 4'-diethylamino-3-hydroxyflavone (FE), 5,6-benzo-4'-diethylamino-3-hydroxyflavone (BFE), and 4´-Diethylamino-3-hydroxy-7-methoxyflavone (MFE) were synthesised as described previously [6, 7, 13]. The chemical structures of these probes and copolymers are shown in Figure 1.

Thin film preparation: The polymer films were required to have a minimum thickness of between 5 and 10 μm, as this is the thickness size required to facilitate adequate loading of therapeutic agents into polymer coatings [21]. The films were cast onto quartz slides (12 mm x 45 mm x 1.5 mm from Lightpath Optical Ltd, UK) yielding dried films of ~10 μm in thickness. The quartz slides were sonicated in deionised water for 15 minutes, washed at least three times with deionised water, acetone, and methanol, and dried in an oven at 70 ºC before use. 5.4 mg of the solid copolymer was dissolved in 137.5 μL of a 5.7 x 10^{-5} M ethanol solution of the requisite probe. The solution was then carefully spread on a quartz slide and the films were cured for 24 hours in a sealed environment with a source of ethanol. The ethanol was present to saturate the atmosphere above the polymer film and help prevent ingress of water into the film during curing. After 24 hours, the copolymer films were removed from the ethanol environment and placed into an oven at 70 ºC for 48 hours to complete the drying process. The films thus obtained were transparent, smooth, and free of any physical inhomogeneities as verified under an optical microscope. The weight ratio of copolymer to fluorophore for the dry films was calculated to be 2230:1 for FE, 1908:1 for BFE, and 2027:1 for MFE, and the corresponding absorbance at λ_{max} never exceeded a value of 0.03.

Spectroscopic measurements: All optical measurements were made at room temperature (~20 ºC) under normal ambient conditions. Steady state fluorescence spectra were obtained using a Cary Eclipse (Varian) spectrophotometer, fitted with a front surface sampling accessory with slits set to 5 nm for emission and 2.5 nm for excitation spectra measurements. Fluorescence lifetimes were recorded using a Time Correlated Single Photon Counting (TCSPC) fluorescence lifetime spectrometer (FluoTime 200, PicoQuant, Germany). Fluorescence was excited using a laser diode with a wavelength of 375 nm, which was pulsed using a PDL-800B laser/LED driver (PicoQuant, Germany) at 20 MHz. The pulsed excitation

light was filtered to remove any spurious long wavelength emissions. Measurements were made at the magic angle (54.7°) with a count rate of less than 1% of the pulse rate to prevent pile-up effects. The instrument response function (IRF) was collected under the same conditions as the sample using a clean quartz slide. Fluorescence lifetimes were extracted from the measured decay curves using the FluoFit program (PicoQuant, Germany), which implements nonlinear least-squares error minimization analysis, based on Simplex and the Levenberg-Marquardt algorithms. The final quoted result was determined by the fit, which had a χ^2 value of less than 1.2 and a residual trace that was symmetric about the zero axes.

Results and discussion

Pyrene fluorescence

Pyrene fluorescence is often used for polarity measurements using the ratio of the first to the third vibronic band of the emission spectrum (I_1/I_3). The changes observed in the spectra are due to dipole-induced dipole interactions based on vibronic coupling [22, 23]. The emission spectra (Figure 2a) show that the shape and position of the vibronic bands in the emission spectra are not affected by the composition of the film and there is also no evidence of an excimer band at 470 nm which implies that emission occurs only from pyrene monomers in the poly(NIPAM-co-NtBA) films. However, a pronounced decrease in the intensity of the first vibronic band with increasing NtBA content in the film is clearly seen. The normalized excitation spectra of pyrene doped films recorded at the emission of the first vibronic band are shown in Figure 2b. As can be seen, the spectra shift to shorter wavelength with increasing NtBA content in the film. The observed vibronic bands at 275, 327, and 340 nm correspond well to reported literature values for dilute solutions [24].

The I_1/I_3 ratio of pyrene (*py* parameter) shows decreases significantly as a function of NtBA content (Figure 2c). According to the pyrene polarity scale, a lower intensity ratio is attributed to a less polar or more hydrophobic environment [22, 25]. Thus, the higher NtBA content causes a reduction in the overall polarity of the film and increases its hydrophobicity. This observation is consistent with results obtained previously using solvatochromic indicators [26]. Using the *py* scale, we can compare polymer polarity (Figure 2d) with liquid solvent data, and this indicates that these polymers have a polarity between that of the aprotic solvents chloroform (*py* = 1.25) and tetrahydrofuran (*py* = 1.35) [22]. However, the situation is not as simple as this, because polarity is a complex parameter. Pyrene being a nonpolar

polyaromatic hydrocarbon means that the predominant mode of interaction with its local environment is dipolarity/polarizability [27], and as a consequence, the *py* scale is relatively insensitive to protic factors [22] which we know are significant for the NIPAM/NtBA copolymers [26]. Dong and Winnik [22] have shown that the *py* parameter for liquid solvents correlates well with the Kamlet-Taft π^* parameter. They noted that the nature of correlation depends on the type of solvents, and for protic aliphatic solvents the following empirical correlation equation was found [22]:

$$py = 0.46 + 1.304\pi^*, \quad n = 9, \; r^2 = 0.964, \; SD = 0.28 \tag{1}$$

A more detailed treatment (Equation 2) that incorporates a solvent polarizability correction term δ and takes into account a hydrogen bond donor ability of solvent (represented by α parameter), was also proposed [22]:

$$py = 0.64 + 1.33(\pi^* - 0.24\delta) - 0.25\alpha, \quad n=32, \; r^2=0.81 \tag{2}$$

where δ is 1 for aromatic, 0.5 for polyhalogenated aliphatic, and 0 for other solvents.

Taking previously reported solvatochromic polarity parameters (note that the average values for π^* and α were used, and $\delta = 0$ in the case of Equation 2), and calculating *py* values it is clear that the polymer case is very different from that which pertains to solvents (Figure 3) [26]. The calculated *py* values are significantly larger than those obtained experimentally and, somewhat surprisingly, the difference between calculated and measured values is larger in the case of the more detailed equation 2. It is worth noting, that similar disagreement between experimental and calculated *py* values (using Equation 2) is also seen for some solvents such as *N*-methylacetamide. For a more accurate picture of polymer polarity (particularly when the structure indicates the potential for hydrogen-bonding) one should also take into consideration all three (α, β, and π*) Kamlet-Taft parameters [26]. If one does this, then one can assess the gross polymer polarity of these films as being closer to the polarity of *N*-methylacetamide (C_3H_7NO on graph), even the *py* value for this solvent (*py* = 1.48 [22]) is significantly larger than those of the polymer film.

In aqueous solutions of pNIPAM (up to ~5 g/L) and its copolymers there is a sharp change in pyrene emission (related to polarity changes) that occurs at the LCST [28-30]. At the LCST, the environment of the pyrene probe changes as the polymer converts to the globular form at higher temperatures. When the fluorescence emission was measured for the pyrene doped, dry films, a pronounced linear decrease in the overall fluorescence intensity with increasing temperature (20 °C to 40 °C) is clearly seen for all the copolymers (Figure 4a,

shows the P65 film as an example) but, interestingly there is no significant change at the LCST. This linear decrease is associated with the fact that the efficiency of the nonradiative processes from the excited state increases with temperature [31]. In figure 4b, we observe that there is also a linear increase in the full width half maximum of the first vibronic band with increasing temperature, and this indicates a small increase in the heterogeneity of the microenvironment. Plotting the changes in intensity of the I_1 and I_3 vibronic bands (Figure 4c for the P65 polymer film), shows that the rate of decrease in intensity was greater for the first vibronic (373.5 nm) band compared to the third band (384.2 nm). Thus it appears that temperature changes in rigid polymer media affects more strongly the $I_1(S_1^{v=0} \rightarrow S_0^{v=0})$ vibronic band transition than the $I_3(S_1^{v=0} \rightarrow S_0^{v=1})$ band and this is probably due to differences in vibronic coupling contributions [23]. Analysis of the excitation spectra monitored at the emission of the first vibronic band of pyrene doped polymer films recorded at various temperatures, indicated that there was no excimer formation associated with these mild experimental conditions [32-38]. Figure 4d shows a plot of the thermally induced changes in the I_1/I_3 ratio (*py* parameter) for the different dry poly(NIPAM-co-NtBA) films. According to this data the polarity of the films decreases linearly with increasing temperature, so that at 40°C the pNIPAM film is only slightly more polar than pNtBA film at 20 °C.

In contrast to the *py* parameter, the solvatochromic Kamlet-Taft $\pi*$ parameter of poly(NIPAM-co-NtBA) copolymers is relatively insensitive to temperature. An increase in temperature from 20 to 40 °C results in small changes in the $\pi*$ value from 0.9 to 0.88 for pNIPAM and from 0.79 to 0.78 for pNtBA [26, 32]. Thus it is clear that, in general, increasing temperature does not significantly affect the polarizability/dipolarity of the NIPAM/NtBA copolymer films. So, if the polarizability is not changing, then another as yet unidentified factor must be causing the changes in the I_1/I_3 ratio. A similar temperature dependence of the I_1/I_3 ratio in solvents has been reported previously [27, 39-40]. In nonpolar, liquid solvents the temperature effect is small, whereas in polar solvents it is more pronounced [39]. However, the nature of this effect is not fully understood [40]. Figure 4e shows the plot of the I_1/I_3 intensity ratio versus temperature for pyrene in ethanol, 1-propanol, pNIPAM film, and pNtBA film. It is apparent from this graph that the slope varies directly with the polarity of the medium, i.e. the highest slope is for ethanol and the lowest for 1-propanol. This data suggests that changes in hydrogen bonding play a more significant role in gross polymer polarity, and therefore the *py* scale is inadequate for accurately characterising gross polymer polarity. In addition, the fact that the magnitude of the I_1/I_3 ratio changes are

small (0.06 to 0.07) for both temperature changes of ~20 °C and the compositional changes makes the *py* scale less suitable for robust analytical characterisation of thin polymer films.

It is also noticeable that there are no significant changes at the LCST of any of the dry copolymer films. This is reasonable to expect since the dried films do not contain water; this means that when the macroscopic structural transition occurs at the LCST, there is no formation of distinct separate (hydrophilic and hydrophobic) phases, and as such the pyrene probe molecules are not physically moved into a new environment. Since the probe molecule environment does not change significantly, there will not be a large change in emission properties [28-30]. This is very different to the pNIPAM in solution where one observes very significant changes in pyrene emission at the LCST [28].

3-HF fluorescence:

In liquid solvents the measurement of FE, MFE, and BFE spectral data, and correlation with physicochemical properties of the solvent are relatively straightforward since the local environment is homogeneous [6, 7, 13]. The polymer case however, is more complex because of structural, energetic, and dynamic microscopic inhomogeneity. In the case of poly(NIPAM-co-NtBA) thermoresponsive polymers, which are random linear copolymers, there is the added possibility of local microscale hydrophilic/hydrophobic microenvironments [18, 19]. The fluorescence emission spectra from all 3-HF fluorophores are strongly dependent on copolymer composition, with increasing hydrophobicity (greater NtBA fraction) leading to a decrease in the ratio between the emission intensity from the N* and T* bands (I_{N*}/I_{T*}) as shown in Figure 5A, 5C, and 5E. The slope of the plot of log (I_{N*}/I_{T*}) vs. copolymer composition does not differ very significantly between FE, MFE, and BFE (Figure 6), but the magnitude of the log (I_{N*}/I_{T*}) is significantly different being lowest for BFE and the largest for FE. These differences in the intensity band ratio of the probes are in line with the data in organic solvents [6, 7, 13].

It is interesting to note that in these spectra, the positions of the N* and T* bands do not vary with copolymer composition, despite the large separation between the bands. The excitation spectra recorded at T* emission are blue shifted with respect to those collected at N* emission (Figure 5B, 5D, and 5F) while in a homogeneous solvent case (ethanol), the excitation spectra are identical for the N* and T* emission bands (data not shown). Furthermore, the excitation spectra recorded at the N* emission band of the probes in

pNIPAM films and pNtBA films are identical indicating that polymer composition has no influence on the N ground and/or excited states. In the T* case, the overlap is not quite as perfect and, while the maxima are the same for pNIPAM and pNtBA, the red edge of the excitation spectra is red-shifted for pNIPAM relative to pNtBA.

When the excitation spectra for all three probes are compared, it is clear that there is very little difference in the separation of the excitation spectra recorded at N* and T* emission bands (ca 10 nm in all three cases), which suggest that the cause of the separation is largely independent of the nature of the probe. We attribute these small differences in the excitation spectra as arising from specific H-bonding interactions between the probe in the ground state and the host polymer matrix. Furthermore, since BFE, unlike FE and MFE, is much less able to form a hydrogen bond between its 4-carbonyl and a protic polymer molecule [13], we can suggest that the observed differences in the excitation spectra are due to H-bonding between the carbonyl group of the polymer and the 3-hydroxy group of the probe. This hydrogen bonding interaction in the ground state may lead to disruption of the intramolecular H-bonding in the 3-HF probes and formation of the new emissive species that do not undergo ESIPT [41]. This is important in the context of developing a quantitative measure for the polarity of the polymer matrix.

Comparing the change in band intensity ratios ($\log(I_{N*}/I_{T*})$) versus the composition of the copolymer (Figure 6) shows a good linear correlation for each of the 3 probes, with pNIPAM being more polar than pNtBA. The NIPAM and NtBA constituents of these copolymers differ only by one methyl group (Figure 1) and this small difference is very difficult to observe using other spectroscopic methods [26]. Thus these probes (with MFE being the most sensitive i.e. largest change in $\log(I_{N*}/I_{T*})$) can be used for polymer composition measurements, for example to plot local composition variations on surfaces. In aprotic liquid solvents, the FE and BFE probes show very similar spectroscopic properties, since there is no hydrogen bonding contribution from the solvent. In protic solvents they show different behaviour, because the intermolecular hydrogen bonding of the solvent with the 4-carbonyl group is sterically hindered in BFE, but not in FE [13]. Therefore, the ordering of the plots in Figure 6 from top to bottom is a result of decreasing H-bonding contribution, with BFE having a much reduced H-bonding ability due to the influence of the additional aromatic ring in its structure (Figure 1). This can be confirmed by correlating the values of $\log(I_{N*}/I_{T*})$ with the solvatochromic parameters of the copolymer films that we have previously reported [26]. Comparison of obtained equations (Equation 3 for FE and

Equation 4 for BFE) clearly indicates that the contribution of hydrogen bonding (α and β parameters) to the value of log (I_{N*}/I_{T*}) is significantly higher for FE then for BFE.

$$\log(I_{N*}/I_{T*}) = 5.853\alpha + 3.086\beta + 0.821\pi* -3, \quad \alpha/\beta = 1.897 \tag{3}$$

$$n = 5, r = 0.999$$

$$\log(I_{N*}/I_{T*}) = 1.763\alpha + 1.091\beta + 0.176\pi* -1, \quad \alpha/\beta = 1.616 \tag{4}$$

$$n = 5, r = 0.997$$

The next step in this study was to attempt to utilize these probes for quantitative polarity measurements. The proposed model for use with these dyes has been developed by Klymchenko and co-workers for use in liquid solvents [7]. It correlates empirically the solvent polarity function $f(\varepsilon)$ with two parameters, the log(I_{N*}/I_{T*}) value and the emission band separation. Plotting these two parameters yields a linear plot in the solvent model, from which $f(\varepsilon)$ of the polymer microenvironment can be then calculated. However, when we investigated the effect of different excitation wavelengths on the 3-HF probe loaded copolymers, we found that the intensity ratio I_{N*}/I_{T*} (Figure 7A-C), and the position of the N* band (Figure 8) varies for every dye. In solvents, this excitation dependence is not observed [32], and so it could be attributed to a classical red-edge effect which is usually observed in rigid media [42-43]. In this case, red-edge excitation will photo-select dielectrically stabilized species, which in turn leads to lower T* emission. However, the excitation wavelength dependence extends over a large range and not just at the red-edge of the excitation spectrum. This indicates that a much more significant interaction is occurring between the fluorophores and the polymer environment. The strong polar nature of these hydrophilic NIPAM-co-NtBA copolymers suggests that it can act as both an H-bond donor and acceptor, which has been measured experimentally [26]. From the fluorescence emission data we can conclude that there is a significant H-bonding interaction between the ground state of the probes and the copolymer matrix. In the case of FE and MFE, we can consider the existence of two ground state species: free and hydrogen-bonded with hydrogen-bonding between the amide hydrogen (N-H groups) of the copolymer and the 4-carbonyl group of the hydroxyflavone fluorophore. Since the absorption spectra of the H-bonded form are red-shifted [44], excitation at the red edge will result in the photo-selection of the H-bonded species. Strongly H-bonded species (of these 3-HF fluorophores) do not undergo ESIPT (or go very slowly), and therefore T*

emission is weaker for these species. Thus, red edge excitation results in a decrease in the T* emission band intensity, yielding a higher I_{N*}/I_{T*} ratio (as observed in Figure 7).

The observed excitation wavelength dependence can be further understood by looking at the BFE case. BFE contains an additional benzene ring, which sterically protects the 4-carbonyl from H-bonding strongly with H-bond donors [13] of the polymer. The systematically lower I_{N*}/I_{T*} ratios observed for BFE compared to FE (Figure 6) is direct evidence that H-bonding of the polymer with the 4-carbonyl of FE is significantly decreased for BFE. We do, however, observe an excitation-dependent emission for BFE, which suggests that an alternate H-bonding interaction between the 3-OH group of the probes and carbonyl oxygen of the copolymers may be occurring driven by the strong H-bond acceptor ability of the copolymers. In liquid organic solvents this type of H-bonding mechanism was not detected for these fluorophores [13]; in a rigid polymer matrix, however, steric interactions may stabilize this particular H-bonded complex, making it emissive. This type of probe-polymer interaction could explain the observed abnormally large separation between the N* and T* bands for such a high I_{N*}/I_{T*} ratio, which does not fit to the linear dependence of $\log(I_{N*}/I_{T*})$ vs. band separation $\upsilon(N^*) - \upsilon(T^*)$ found for organic solvents (Figure 9). Since the polymer data do not fit this relationship, it is not practical to use these probes for quantitative polarity measurements as demonstrated for solvents [7]. This strong upward deviation for the polymers represents the "low efficiency ESIPT" case where the hydrogen bonding between the polymer and the probe disrupts the intramolecular hydrogen bonding, thus uncoupling the ESIPT process, without significant effect on the energy of the N* and T* states.

Fluorescence lifetime measurements

The fluorescence lifetimes of these probes in the copolymers were measured to provide more fundamental information on the ESIPT process in these heterogeneous copolymer environments. The fluorescence decays for all of the probes in the polymer matrices are complex (Tables 1-3), with the N* bands containing 3 terms and the T* band containing 2 or 3 terms. For all three 3-HF dyes, a fast decay component, τ_1, of ~ 10 – 100 ps with relatively high positive amplitude, corresponding to the ESIPT process, is observed at the emission of the N* band. The lifetime of this component becomes significantly longer (~0.2 –0.5 ns) and of negative amplitude at the emission of the T* band for the FE and MFE probes [Tables 1 & 2]. This indicates that the T* state is generated from the N* state through

a slow and non-reversible ESIPT process. The fact that the other two decay components, τ_2 and τ_3 of the T* state are significantly longer than the corresponding components of the N* state provide further evidence that the ESIPT process is irreversible. Figure 10 shows the intensity-averaged lifetime ($\overline{\tau}$) [42] data obtained for all 3 dyes in each of the dry copolymer films. None of the fluorophores show any significant changes in $\overline{\tau}$ with changes in copolymer composition at the emission wavelengths corresponding to the N* or T* bands, or over the full emission range. There are, however, very significant differences in lifetime between the N* and T* emission bands. In aprotic solvents, such as ethyl acetate and dichloromethane, the lifetimes for the N* and T* bands are equal, which indicates that ESIPT is a fast, reversible two-state process [45]. In this copolymer system this is not the case and the significant lifetime difference indicate a non-reversible ESIPT system. This is obviously due to the hydrogen bonding interactions between the polymer and the excited N* and T* species. A similar effect was observed in the parent 3-hydroxyflavones in protic solvents where solvent hydrogen bonding with the dye may increase the activation energy barrier to ESIPT [46-47]. In this case, ESIPT is irreversible and is characterized by the fact that the average lifetime of the T* band is longer than that for the N* band [43-44]. The highest degree of ESIPT non-equilibration seems to occur in MFE doped copolymers where the difference in average lifetime ($\Delta\tau$) is $\approx$ 1.6 ns (Table 1), while the BFE doped copolymers have a much lower $\Delta\tau$ of $\approx$ 0.4 ns) (Table 3 and Figure 10A-C). This supports the argument that the interaction is at least partly due to hydrogen bonding effects, since the BFE probe is inherently less suitable for hydrogen bonding at the carbonyl group due to the presence of the additional aromatic ring.

Conclusions

Pyrene emission shows a good linear correlation with copolymer composition for these copolymers, with a ~6% decrease in the ratio of the intensities of I_1 and I_3 vibronic bands on going from 100% NIPAM to 100% NtBA. However, the I_1/I_3 ratio was found to exhibit rather poor correlation with measured solvatochromic polarity parameters [24], using established correlation equations. This is because the "polarity" sensed by pyrene is related only to dipole-induced dipole interactions based on vibronic coupling [23], and essentially ignores hydrogen bonding effects. This is crucial because one cannot ignore the significant effects induced by H-bonding on probe environments. Another factor which makes pyrene less attractive as a probe is the sensitivity of the I_1/I_3 ratio to temperature, where we observe a

~5% change in the I_1/I_3 ratio going from 20 to 40 ºC. This strong temperature dependence may lead to misinterpretation of pyrene fluorescence data unless strict temperature control is enforced. Furthermore, from careful examination of the data it is clear that physiochemical changes that occur at the LCST do not affect pyrene emission significantly. All of these observations suggest that pyrene is therefore not a good probe for the robust measurement of gross polarity in hydrophilic polymers.

For the fluorescent 3-hydroxyflavone derivatives studied it is clear that they can be used to measure changes in the chemical composition of random-linear, hydrophilic/hydrophobic thermoresponsive copolymer films. However, these particular probes cannot be used for quantitative polarity measurements of hydrophilic polymers (using simple emission parameters such as $\log(I_{N*}/I_{T*})$), in a manner analogous to solvents because of heterogeneity in the ground state hydrogen-bonding and the non-reversible nature of the ESIPT process, which are evidenced by excitation wavelength dependence and a difference in the fluorescence lifetimes of the N* and T* bands [7, 45]. Further studies are underway to explore how the gross polarity of the heterogeneous microenvironment of hydrophilic thermoresponsive copolymer films might be better measured using 3-hydroxyflavone fluorophores.

References:

[1]   H. Bult, (2000), Restenosis: a challenge for pharmacology, *Trends Pharmacol. Sci.* **21**(7), 274–279.

[2]   A. L. Lewis, L. A. Tolhurst, and P. W. Stratford, (2002), Analysis of a phosphorylcholine-based polymer coating on a coronary stent pre- and post-implantation, *Biomaterials*, **23**(7), 1697–1706.

[3]   M. S. Paley, R. A. McGill, S. C. Howard, S. E. Wallace, and J. M. Harris, (1990), Solvatochromism - a new method for polymer characterization, *Macromolecules*, **23**(21), 4557–4564.

[4]   S. Spange, E. Vilsmeier, K. Fischer, A. Reuter, S. Prause, Y. Zimmermann, and C. Schmidt, (2000), Empirical polarity parameters for various macromolecular and related materials, *Macromol. Rap. Commun.* **21**(10), 643–649.

[5]   A. S. Klymchenko, T. Ozturk, V. G. Pivovarenko, and A. P. Demchenko, (2001), A 3-hydroxychromone with dramatically improved fluorescence properties, *Tetrahedron Lett.* **42**(45), 7967–7970.

[6]   A.S. Klymchenko, V.G. Pivovarenko, T. Ozturk, and A.P. Demchenko, (2003) Modulation of the solvent-dependent dual emission in 3-hydroxychromones by substituents, *New J. Chem.*, **27**(9), 1336–1343.

[7]   A. S. Klymchenko and A. P. Demchenko, (2003), Multiparametric probing of intermolecular interactions with fluorescent dye exhibiting excited state intramolecular proton transfer, *Phys. Chem. Chem. Phys.* **5**(3), 461–468.

[8]   P.T. Chou, M.L. Martinez, J.H. Clements, (1993), Reversal of excitation behavior of proton-transfer vs. charge-transfer by dielectric perturbation of electronic manifolds, *J. Phys. Chem.*, **97**(11), 2618–2622.

[9]   A.S. Klymchenko and A.P. Demchenko, (2002), Electrochromic Modulation of Excited-State Intramolecular Proton Transfer: the New Principle in Design of Fluorescence Sensors, *J. Am. Chem. Soc.*, **124**(41), 12372–12379.

[10]   A. P. Demchenko, S. Ercelen, A. D. Roshal, and A. S. Klymchenko, (2002), Excited-state proton transfer reaction in a new benzofuryl 3-hydroxychromone derivative: The influence of low-polar solvents, *Polish J. Chem.* **76**(9), 1287–1299.

[11]   S. Ercelen, A. S. Klymchenko, and A. P. Demchenko, (2002), Ultrasensitive fluorescent probe for the hydrophobic range of solvent polarities, *Anal. Chim. Acta*, **464**(2), 273–287.

[12] A. S. Klymchenko, Y. Mely, A. P. Demchenko, and G. Duportail, (2004), Simultaneous probing of hydration and polarity of lipid bilayers with 3-hydroxyflavone fluorescent dyes, *BBA-Biomembranes*, **1665**(1–2), 6–19.

[13] A. S. Klymchenko, V. G. Pivovarenko, and A. P. Demchenko, (2003), Elimination of the hydrogen bonding effect on the solvatochromism of 3-hydroxyflavones, *J. Phys. Chem. A.* **107**(21), 4211–4216.

[14] A.S. Klymchenko, G. Duportail, Y. Mely, and A.P. Demchenko, (2003). Ultrasensitive Two-Color Fluorescence Probes for Dipole Potential in Phospholipid Membranes, *Proc. Natl. Acad. Sci USA*, **100**(20), 11219–11224.

[15] A. G. Ryder, B. Szczupak, Y. A. Rotchev, A. S. Klymchenko, A. Gorelov, and T. J. Glynn, (2005), A fluorescence methodology for assessing the polarity and composition of novel thermoresponsive hydrophilic/hydrophobic copolymer system, *Proc SPIE – Int. Soc. Opt. Eng.* **5826**, 1–11.

[16] K. B Doorty, T. A. Golubeva, A. V Gorelov, Y. A. Rochev, L. T. Allen, K. A. Dawson, W. M. Gallagher, and A. K. Keenan, (2003), Poly(N-isopropylacrylamide) co-polymer films as potential vehicles for delivery of an antimitotic agent to vascular smooth muscle cells, *Cardiovasc. Path.* **12**(2), 105–110.

[17] Y. Rochev, T. Golubeva, A. Gorelov, L. Allen, W. M. Gallagher, I. Selezneva, B. Gavrilyuk, and K. Dawson, (2001), Surface modification for controlled cell growth on copolymers of N-isopropylacrylamide, *Progr. Colloid. Polym. Sci.*, **118**, 153–156.

[18] I. Lynch, I. A. Blute, B. Zhmud, P. MacArtain, M. Tosetto, L. T. Allen, H. J. Byrne, G. F. Farrell, A. K. Keenan, W. M. Gallagher, and K. A. Dawson, (2005), Correlation of the adhesive properties of cells to N-Isopropylacrylamide/N-tert-Butylacrylamide copolymer surfaces with changes in surface structure using contact angle measurements, molecular simulations, and Raman spectroscopy, *Chem. Mater.* **17**(15), 3889–3898.

[19] Y. Rochev, D. O. Halloran, T. Gorelova, V. Gilcreest, I. Selezneva, B. Gavrilyuk, and A. Gorelov, (2004), Rationalising the design of polymeric thermoresponsive biomaterials, *J. Mater. Sci.-Mater. M.*, **15**(4), 513–517.

[20] V. P. Gilcreest, W. M. Carroll, Y. A. Rochev, I. Blute, K. A. Dawson, and A. V. Gorelov, (2004), Thermoresponsive poly(N-isopropylacrylamide) copolymers: Contact angles and surface energies of polymer films, *Langmuir*, **20**(23), 10138–10145.

[21] K. al-Lamee and D. Cook, (2003), Polymer coating techniques for drug-eluting stents, *Medical Device Technology*, **14**, 12–14.

[22] D. C. Dong and M. A. Winnik, (1984), The Py scale of solvent polarities, *Can. J. Chem.* **62**, 2560–2565.

[23] D. S. Karpovich and G. J. Blanchard, (1995), Relating the polarity-dependent fluorescence response of pyrene to vibronic coupling. Achieving a fundamental understanding of the *py* polarity scale, *J. Phys. Chem.* **99**(12), 3951–3958.

[24] G. Duportail and P. Lianos, (1990), Phospholipid-vesicles treated as fractal objects - a fluorescence probe study, *Chem. Phys. Lett.* **165,** 35–40.

[25] J. K. Thomas, (1987), Characterization of surfaces by excited-states. *J. Phys. Chem.* **91,** 267–276.

[26] B. Szczupak, A. G. Ryder, D. M. Togashi, Y. A. Rotchev, A. Gorelov, and T. J. Glynn, (2009), Measuring the micro-polarity and hydrogen-bond donor/acceptor ability of thermoresponsive *N*-isopropylacrylamide/*N*-tert-butylacrylamide copolymer films using solvatochromic indicators, *Appl. Spectrosc.* **63**(4), 442–449.

[27] D. Arrais and J. Martins, (2007), Bilayer polarity and its thermal dependency in the ℓ_o and ℓ_d phases of binary phosphatidylcholine/cholesterol mixtures, *Biochim. Biophys. Acta, Biomembr.* **1768**(11)**,** 2914–2922.

[28] F. M. Winnik, (1990), Fluorescence Studies of Aqueous Solutions of Poly(N-isoproylacrylamide) below and above their LCST, *Macromolecules,* **23,** 233–242.

[29] H. G. Schild, (1992), Poly(N-isopropylacrylamide): experiment, theory and application, *Prog. Polym. Sci.* **17,** 163–249.

[30] H. Ringsdorf, J. Venzmer, and F. M. Winnik, (1991), Fluorescence studies of hydrophobically modified poly(N-isopropylacrylamides), *Macromolecules,* **24,** 1678–1686.

[31] T. D. Martins, S. B. Yamaki, E. A. Prado, and T. D. Z. Atvars, (2003), Broadening of the fluorescence spectra of hydrocarbons in ethylene-vinyl acetate copolymers and the dynamics of the glass transition, *J. Photochem. Photobiol. A.* **156,** 91–103.

[32] Szczupak B (2003), Evaluation of polarity and hydrogen bonding ability of thermoresponsive N-isopropylacrylamide/N-tert-butylacrylamidecopolymer films using solvatochromic and fluorescence probes. PhD thesis, National University of Ireland, Galway, Galway.

[33] K. Mizuno and A. Matsui, (1987), Competition and coexistence of free and self-trapped excitons in aromatic molecular-crystals, *J. Lumin.* **38,** 323–325.

[34] A. Matsui, T. Ohno, K. Mizuno, T. Yokoyama, and M. Kobayashi, Effect of hydrostatic-pressure on excitons in alpha-perylene crystals. *Chem. Phys.,* **111,** 121–128, (1987).

[35] R. Seyfang, H.C. Port, and J. Wolf, Picosecond study on excimer formation in pyrene single-crystals.2. the excimer precursor state in the high-temperature phase. *J. Lumin.,* **42,** 127–135, (1988).

[36] R. Seyfang, H.Port, P. Fischer, and H. C. Wolf, (1992), Picosecond study on excimer formation in pyrene crystals. 3. complete analysis of the high-temperature phase between 5 and 300-K. *J. Lumin.* **51,** 197–208.

[37] O. E. Zimerman and R. G. Weiss, (1998), Static and dynamic fluorescence from alpha,omega-Di(1-pyrenyl)alkanes in polyethylene films. Control of probe conformations and information about microstructure of the media, *J. Phys. Chem. A.* **102**(28), 5364–5374.

[38] E. A. Prado, S. B. Yamaki, T. D. Z. Atvars, O. E. Zimerman, and R. G. Weiss, (2000), Static and dynamic fluorescence of pyrene as probes of site polarity and morphology in ethylene-co-(vinyl acetate) (eva) films, *J. Phys. Chem. B,* **104,** 5905–5914.

[39] R. Waris, W. E. Acree Jr., and K. W. Street Jr., (1988), The Py and BPe polarity scales: effect of temperature of pyrene and benzo[ghi]perylene fluorescence spectra, *Analyst,* **113**(9), 1465–1467.

[40] Chen, S. and McGuffin, V.L. (1994) Temperature effect on pyrene as a polarity probe for supercritical fluid and liquid solutions. *Appl. Spectrosc.,* **48**(5)**,** 596-603.

[41] A. S. Klymchenko and A. P. Demchenko, (2002), Probing AOT reverse micelles with two-color fluorescence dyes based on 3-hydroxychromone, *Langmuir* **18**(15), 5637–5639.

[42] B. Valeur (2002) *Molecular Fluorescence, Principles and Applications*, Wiley-VCH, GmbH.

[43] A.P. Demchenko, (2002), The red-edge effects: 30 years of exploration, *Luminescence*, **17**, 19–42.

[44] V. V. Shynkar, A. S. Klymchenko, E. Piémont, A. P. Demchenko, and Y. Mély, (2004), Dynamics of intermolecular hydrogen bonds in the excited states of 4 '-dialkylamino-3-hydroxyflavones. On the pathway to an ideal fluorescent hydrogen bonding sensor, *J. Phys. Chem. A*. **108**(40), 8151–8159.

[45] V. V. Shynkar, Y. Mély, G. Duportail, E. Piémont, A. S. Klymchenko, and A. P. Demchenko, (2003), Picosecond time-resolved fluorescence studies are consistent

with reversible excited-state intramolecular proton transfer in 4'-dialkylamino-3-hydroxyflavones, *J. Phys. Chem. A.* **107**(45), 9522–9520.

[46] A. J. G. Strandjord, P. F. Barbara, (1985), Proton-Transfer Kinetics of 3-Hydroxyflavone: Solvent Effects, *J. Phys. Chem.* **89**, 2355–2361.

[47] D. A. Yushchenko, V. V. Shvadchak, A. S. Klymchenko, G. Duportail, V. G. Pivovarenko, and Y. Mely, (2007), Modulation of excited-state intramolecular proton transfer by viscosity in protic media, *J. Phys. Chem. A*. **111**(40), 10435–10439.

Figure Captions

Figure 1: Chemical structures of : **(a)** the NIPAM-co-NtBA copolymers showing the very small structural difference of one methyl group between the NIPAM and NtBA groups, (b) the flavone based fluorophores 4'-diethylamino-3-hydroxyflavone (FE), 5,6-benzo-4'-diethylamino-3-hydroxyflavone (BFE), and 4´-diethylamino-3-hydroxy-7-methoxyflavone (MFE)) used in this study.

Figure 2 **(a)** Normalized emission spectra of pyrene doped poly(NIPAM-co-NtBA) films, **(b)** normalized excitation spectra of pyrene doped poly(NIPAM-co-NtBA) films recorded at the emission of the first vibronic band, **(c)** the *py* values for poly(NIPAM-co-NtBA) films at 20 ºC, and **(d)** categorization of poly(NIPAM-co-NtBA) films along the *py* solvent polarity scale. The *py* values for solvents were taken from Ref. [34].

Figure 3: Plot of measured *py* versus calculated values for poly(NIPAM-co-NtBA) films, (□) Py values obtained from Equation 1, (o) *py* values obtained from Equation 2.

Figure 4: Temperature dependence of: **(a)** integrated fluorescence intensity, and **(b)** the full width at half maxima (FWHM) of pyrene doped P65 copolymer film. **(c)** Temperature dependence of the intensity of the first (I_1) and the third (I_3) vibronic band of pyrene doped P65 copolymer film. Intensities normalized to the emission at 20°C. **(d)** Temperature dependence of the I_1/I_3 ratio (*py* parameter) of pyrene doped poly(NIPAM-co-NtBA) films ((□) pNtBA, (o) P50, (Δ) p65, (◊) p85, (∇) pNIPAM). **(e)** Comparison of the temperature dependence of the I_1/I_3 ratio as a function of temperature for :(o) ethanol, (Δ) 1-propanol, (∇) pNIPAM, and (□) pNtBA. Data for ethanol and 1-propanol from Ref. [27].

Figure 5: Normalized fluorescence spectra (**a, c, e**) and excitation spectra (**b, d, f**) of hydroxyflavone FE (**a** & **b**), MFE (**c** & **d**), and BFE (**e** & **f**) doped copolymers. (**a, c, e**): NIPAM (Δ), P85 (○), P65 (□), P50 (∇), NtBA (◊), excitation wavelength 375 nm. (**b, d, f**): excitation spectra of NIPAM (Δ), (⩕) and NtBA (◊),(⊗) recorded at maximum of N* (Δ),(◊) and T* (⩕),(⊗) band.

Figure 6: Plot of log (I_N*/I_T*) versus % of hydrophilic component NtBA for the hydroxyflavone FE (Δ), (MFE (□), BFE (◯)) doped films, using a 375 nm excitation wavelength.

**Figure 7:** Dependence of emission band ratio log(I_{N*}/I_{T*}) on excitation wavelength for MFE (**A**), FE (**B**), and BFE (**C**), and NIPAM (Δ), P85 (○), P65 (□), P50 (▽), NtBA (◊).

Figure 8: Position of N* band maxima in NIPAM-NtBA copolymer system (50% NtBA case) as a function of excitation wavelength.

Figure 9: Plot of the log(I_{N*}/I_{T*}) ratio of dye FE (▲) and BFE (Δ) vs. band separation ν_{N*} - ν_{T*} in different organic solvents based on the data from Ref. [7]. Filled circles (●) correspond to the data from FE in pNIPAM (1) and pNtBA (2). Empty circles (○) correspond to the data from BFE in pNIPAM (1) and pNtBA (2). Solid lines represents linear fits for the liquid organic solvents.

Figure 10: Average fluorescence lifetime ($\overline{\tau}$) of FE (A), BFE (B), and MFE (C) doped copolymers measured at N* band maximum (□), T* band maximum (○), and all emission wavelengths (Δ), using a 410 nm long pass filter.

Figure 1

FE   MFE   BFE
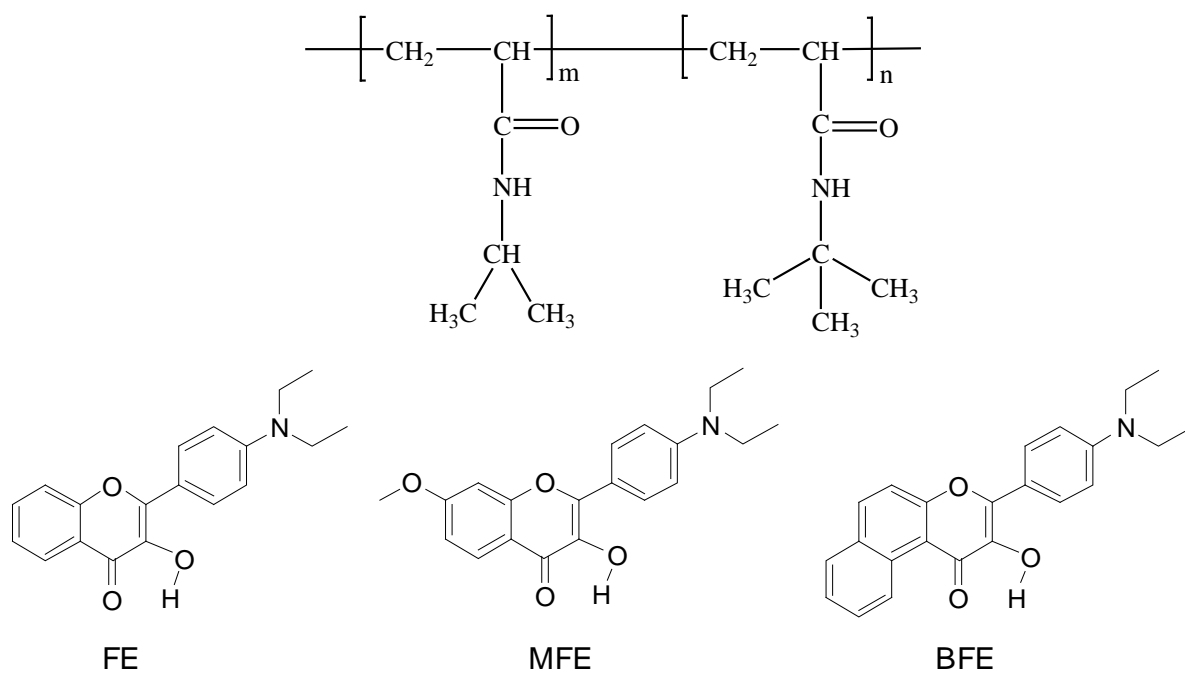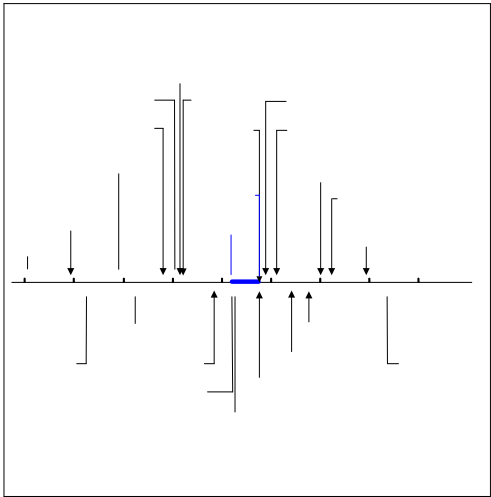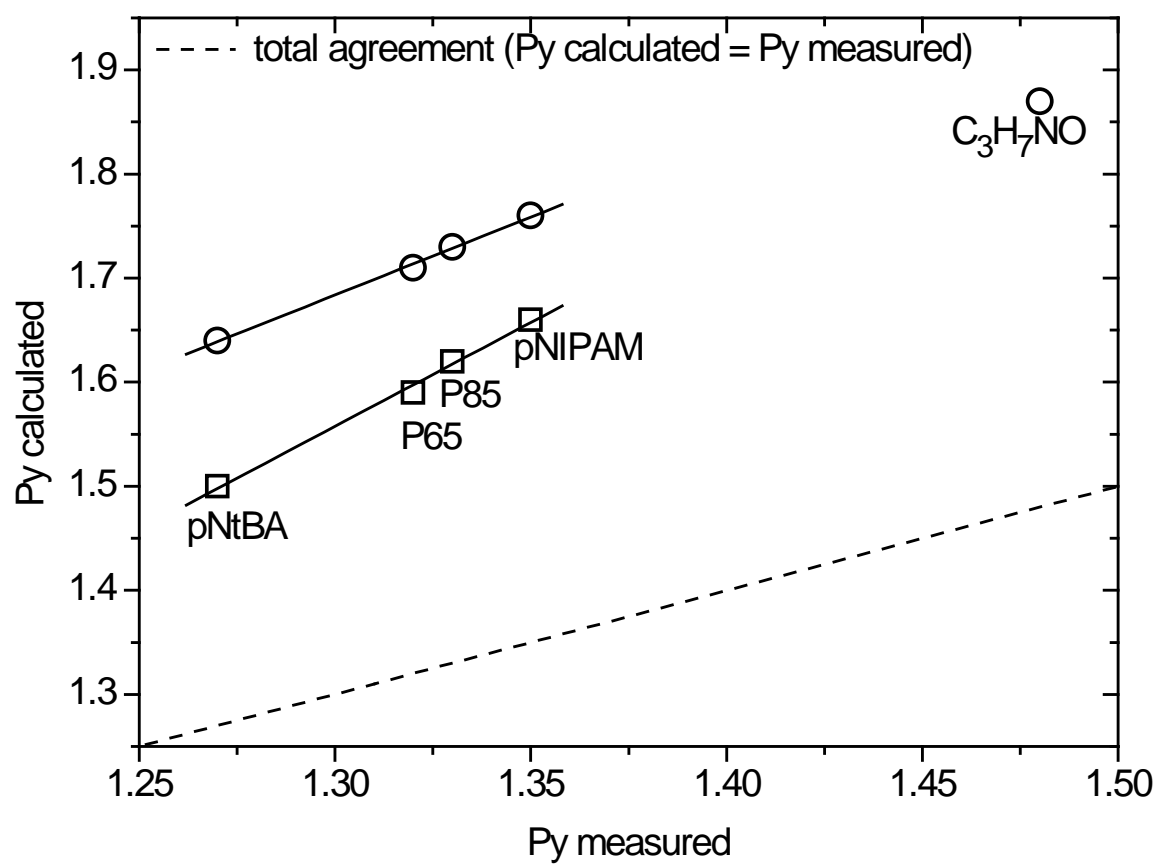
Figure 2
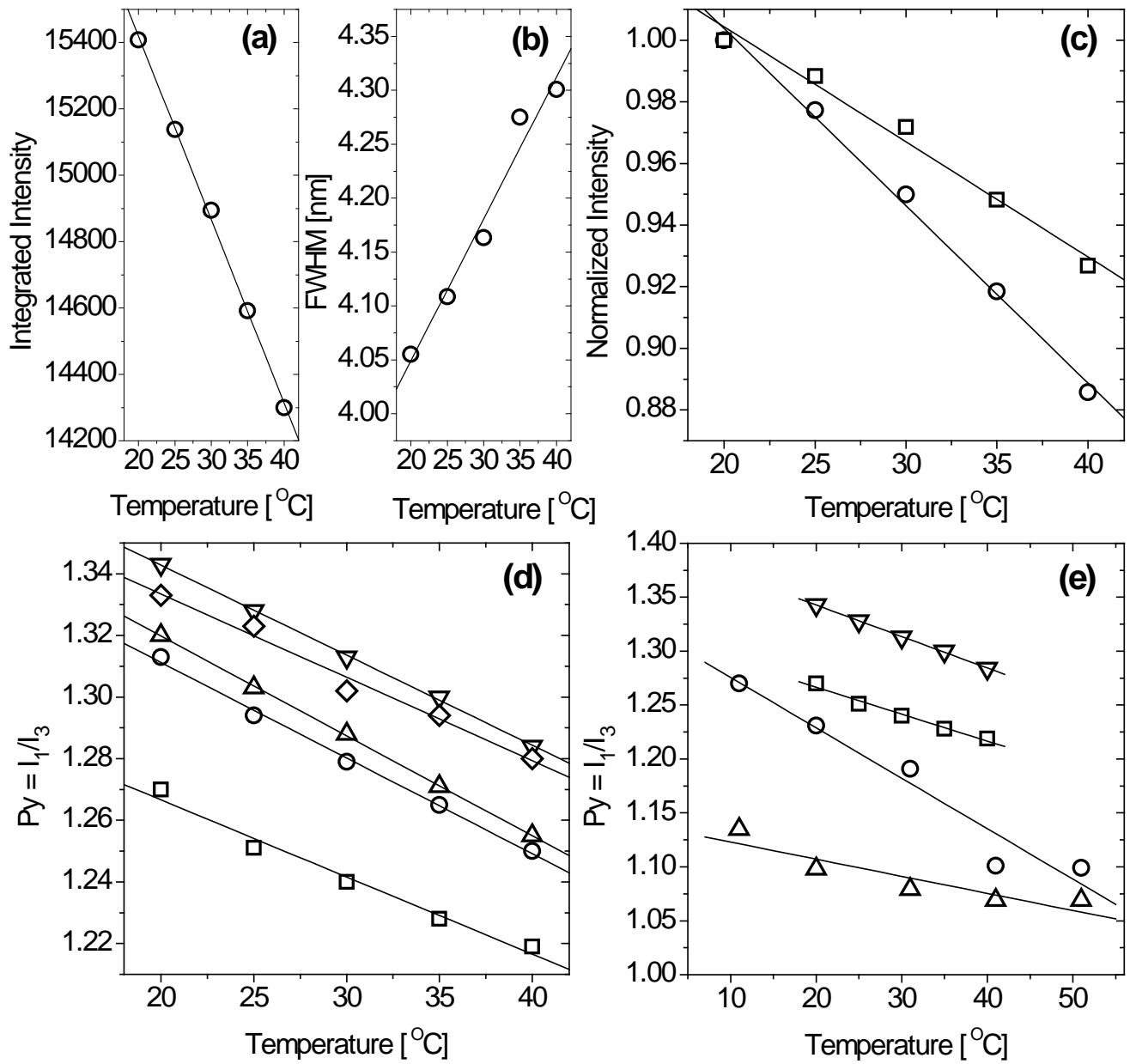
Figure 3

Figure 4

Figure 5
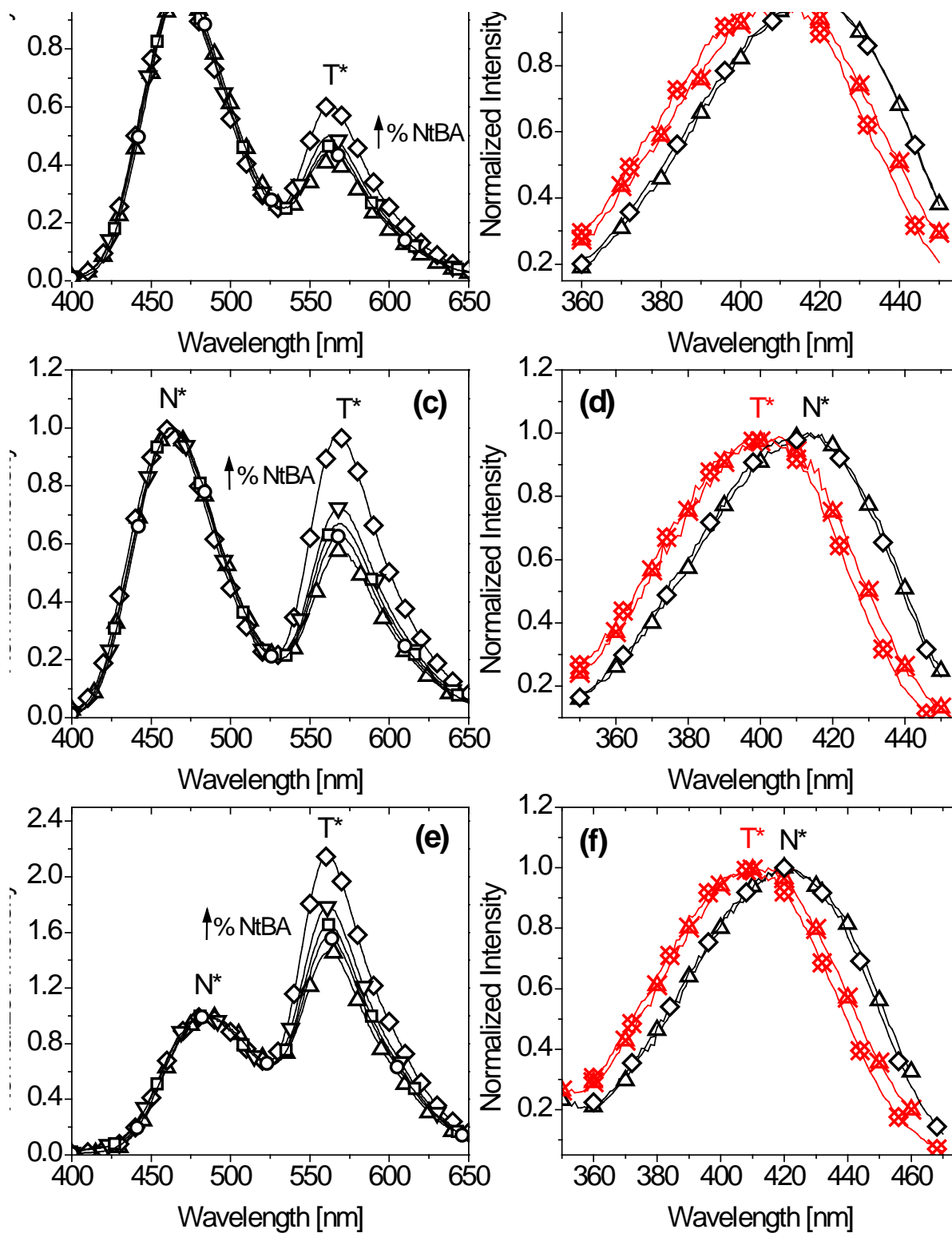
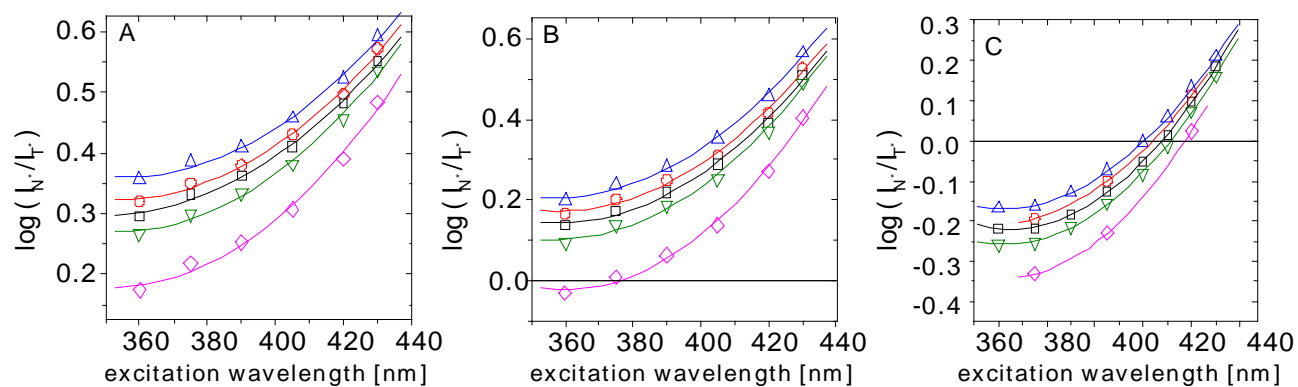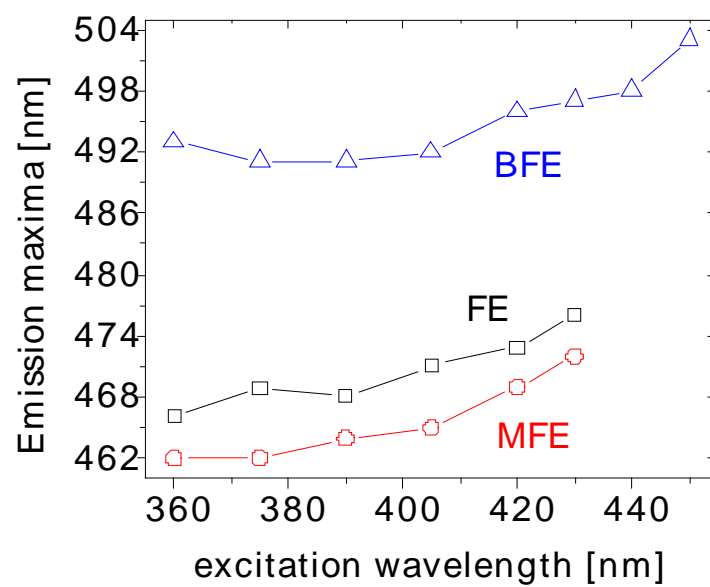**Figure 6**
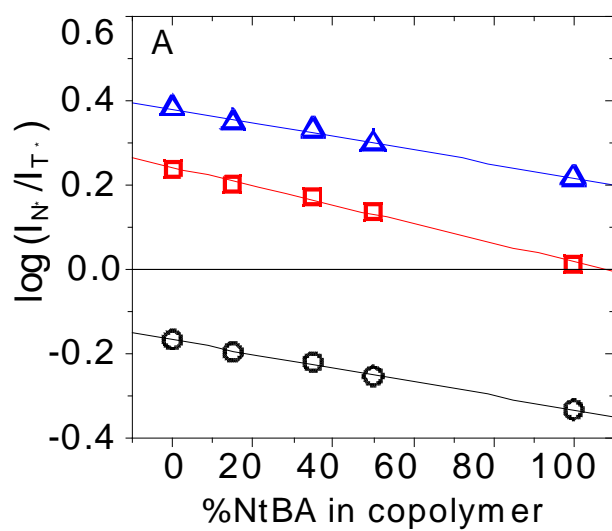
Figure 7

Figure 8

Figure 9

Figure 10

Table 1: Fluorescence lifetime analysis data for **MFE** incorporated into dry poly(NIPAM-co-NtBA) films. Excitation wavelength 375 nm. Errors in brackets (±) are calculated from support plane analysis.

Sample	Band	$\alpha_1{}^b$	τ_1 (ns)	$\alpha_2{}^b$	τ_2 (ns)	$\alpha_3{}^b$	τ_3 (ns)	$\overline{\tau}$ (ns)	χ^2
pNIPAM	N*	0.57	0.05 (±0.04)	0.16	0.67 (±0.17)	0.27	2.13 (±0.10)	1.83	1.03
	T*	-0.1	0.37 (±0.20)	0.41	2.54 (±1.6)	0.49	3.92 (±0.43)	3.47	1.15
P85	N*	0.81	0.01	0.08	0.71 (±0.14)	0.11	2.20 (±0.10)	1.85	1.22 [a]
	T*	-0.12	0.50 (±0.27)	0.22	1.79 (±1.33)	0.67	3.61 (±0.18)	3.42	1.16
P65	N*	0.7	0.03	0.13	0.70 (±0.26)	0.17	2.18 (±0.16)	1.82	1.3 [a]
	T*	-0.09	0.50 (±0.37)	0.18	1.74 (±1.43)	0.73	3.61 (±3.14)	3.48	1.15
P50	N*	0.4	0.11 (±0.07)	0.26	0.83 (±0.21)	0.34	2.31 (±0.14)	1.91	1.13
	T*	-0.08	0.29 (±0.20)	0.54	2.78 (±1.68)	0.38	4.20 (±0.62)	3.54	1.12
pNtBA	N*	0.53	0.07 (±0.05)	0.18	0.67 (±0.20)	0.29	2.23 (±0.12)	1.9	1.07
	T*			0.55	2.76 (±0.96)	0.45	4.28 (±0.60)	3.61	1.09

[a] χ^2 values are high at > 1.2, however, fit was not improved by using next more complex model.

[b] $\alpha_1 \alpha_{,2}$ and α_3 values were normalized according to $\left|\alpha_1\right| + \left|\alpha_2\right| + \left|\alpha_3\right| = 1$
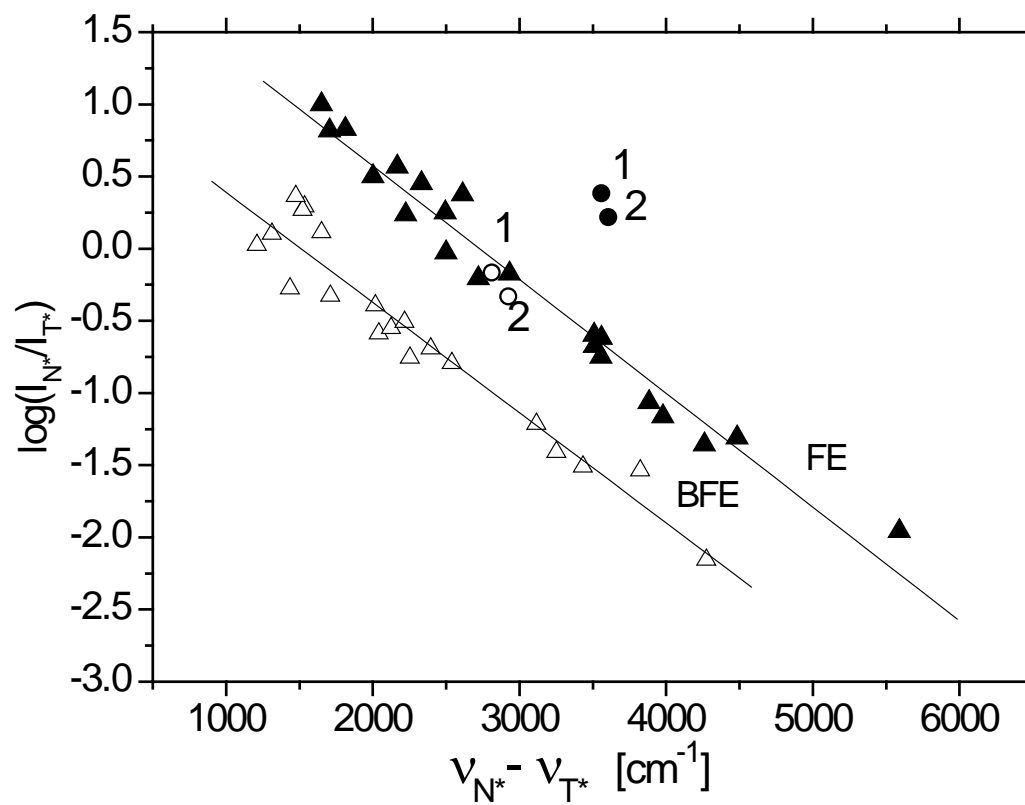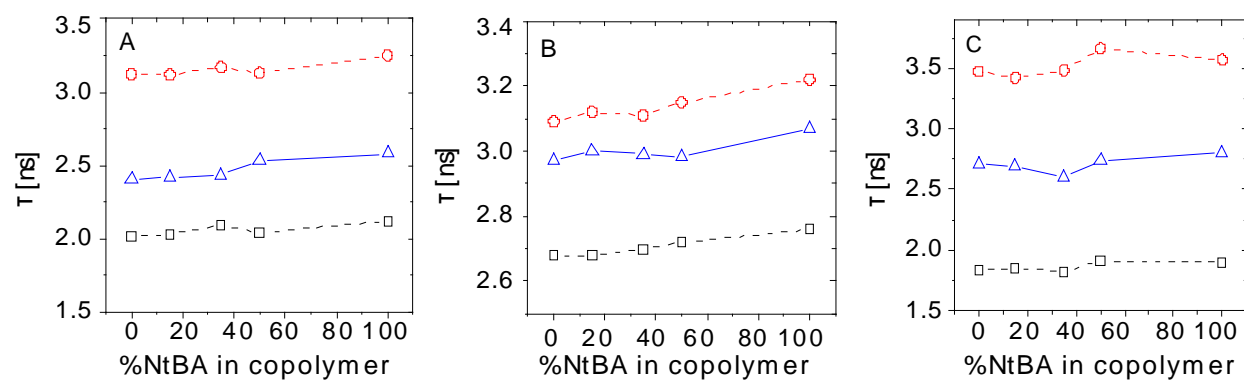
Table 2: Fluorescence lifetime analysis data for **FE** incorporated into dry poly(NIPAM-co-NtBA) films. Excitation wavelength 375 nm. Errors in brackets (±) are calculated from support plane analysis.

Sample	Band	$\alpha_1{}^b$	τ_1 (ns)	$\alpha_2{}^b$	τ_2 (ns)	$\alpha_3{}^b$	τ_3 (ns)	(ns)	χ^2
NIPAM (0 % of NtBA)	N*	0.59	0.04	0.16	0.88 (±0.36)	0.25	2.36 (±0.08)	2.01	1.09
	T*	- 0.15	0.25 (±0.12)	0.25	1.94 (±1.23)	0.6	3.36 (±0.24)	3.12	1.12
P85 (15 % of NtBA)	N*	0.38	0.09	0.22	0.86 (±0.26)	0.4	2.34 (±0.13)	2.03	1.15
	T*	- 0.11	0.29 (±0.16)	0.32	2.03 (±1.08)	0.58	3.43 (±1.83)	3.12	1.16
P65 (35 % of NtBA)	N*	0.4	0.08	0.21	0.9 (±0.3)	0.39	2.41 (±0.16)	2.09	1.14
	T*			0.49	2.47 (±0.86)	0.51	3.62 (±0.39)	3.17	1.12
P50 (50 % of NtBA)	N*	0.38	0.09	0.24	0.84 (±0.20)	0.38	2.38 (±0.08)	2.04	0.97
	T*	- 0.09	0.31 (±0.23)	0.26	1.71 (±0.92)	0.65	3.39 (±0.55)	3.13	1.18
NtBA (100 % of NtBA)	N*	0.32	0.20 (±0.14)	0.31	1.22 (±0.64)	0.37	2.6 (±1.12)	2.12	1.28 [a]
	T*			0.43	2.12 (±0.39)	0.57	3.72 (±0.42)	3.25	1.13

[a] χ^2 values are high at > 1.2, however, fit was not improved by using next more complex model.

[b] α_1, α_2 and α_3 values were normalized according to $|\alpha_1| + |\alpha_2| + |\alpha_3| = 1$

Table 3: Fluorescence lifetime analysis data for **BFE** incorporated **into dry** poly(NIPAM-co-NtBA) films. Excitation 375 nm. Errors in brackets (±) are calculated from support plane analysis.

Sample	Band	α_1[b]	τ_1 (ns)	α_2[b]	τ_2 (ns)	α_3[b]	τ_3 (ns)	$\bar{\tau}$ (ns)	χ^2
pNIPAM	N*	0.4	0.09	0.17	1.12 (±0.48)	0.42	2.98 (±0.19)	2.68	1.08
	T*	-	-	0.18	1.15 (±0.39)	0.82	3.25 (±0.10)	3.09	1.28[a]
P85	N*	0.39	0.1	0.15	1.11 (±0.77)	0.46	2.93 (±0.29)	2.68	1.2
	T*	-	-	0.16	1.08 (±0.43)	0.84	3.25 (±0.11)	3.12	1.09
P65	N*	0.53	0.05	0.12	1.02 (±0.55)	0.36	2.96 (±0.18)	2.7	1.15
	T*	0.66	0.02	0.05	1.32 (±0.84)	0.29	3.28 (±0.29)	3.11	1.18
P50	N*	0.28	0.14	0.19	1.23 (±1.19)	0.53	3.0 (±1.26)	2.72	1.11
	T*	0.32	0.05	0.1	1.32 (±0.46)	0.57	3.31 (±0.20)	3.15	1.16
pNtBA	N*	0.34	0.12 (±0.11)	0.17	1.30 (±0.72)	0.48	3.05 (±0.48)	2.76	1.03
	T*	-	-	0.15	1.01 (±0.46)	0.85	3.34 (±0.11)	3.22	1.14

[a] χ^2 values are high at > 1.2, however, fit was not improved by using next more complex model.

[b] α_1, α_2 and α_3 values were normalized according to $|\alpha_1| + |\alpha_2| + |\alpha_3| = 1$